PERGAMON

Computers and Structures 77 (2000) 141–154

Computers & Structures

www.elsevier.com/locate/compstruc

Variable singularity boundary element and its applications in computation of SIFs

N.K. Mukhopadhyay[a,*], S.K. Maiti[b], A. Kakodkar[a]

[a] *Reactor Design and Development Group, Bhabha Atomic Research Centre, Mumbai 400 085, India*
[b] *Mechanical Engineering Department, Indian Institute of Technology, Mumbai 400 076, India*

Received 11 November 1998; accepted 7 September 1999

Abstract

Two boundary elements have been proposed for simulation of variable order singularities in two dimensions. The first can model the variable order strain singularity near a crack tip and the second can simulate both the strain and traction. These elements can be easily incorporated in a standard boundary element computer programme. The elements are useful for computation of stress intensity factors (SIFs) in fracture mechanics. To improve the accuracy of such computations further, a modified crack closure integral (MCCI) based method for mechanical loading are presented. Examples of mode I and mixed mode crack problems are examined to illustrate the performance of the proposed elements and the MCCI based calculations. The effects of order of Gauss quadrature associated with such elements on the accuracy of the SIFs are also reported.

Keywords: Variable order strain singularity; Variable order traction singularity; Boundary element; Mechanical loading on crack; Modified crack closure integral; Stress intensity factor; Accuracy of SIF computation

1. Introduction

There are situations where the order of singularity at a point in a given domain is variable. In the case of stress analysis, a kinked crack is a typical example. The order of singularity at the knee varies with the knee angle [1]. Another example from the same area is that of a crack terminated at a bimaterial interface. The order of singularity at the crack tip lying on the interface varies with the material combinations and the state of stress, i.e. plane stress or plane strain [2]. There are a host of finite elements, e.g. Tracey and Cook [3], Stern [4], Maiti [5], etc., just to mention a few, which can help to model such problems. These elements are based on either the displacement or hybrid formulation. The hybrid formulation is mathematically elegant, permits direct computation of stress intensity factors (SIFs) and provides high accuracy, even when a small number of such elements is used around the crack tip. The displacement formulation is more simple and widely used. In the standard boundary element method (BEM) [6–8], the most common square root singularity has been at the centre of focus and the problem of variable order singularity has not received, to our knowledge, any attention. There is therefore a need to develop elements to be useful in such applications. This paper mainly focusses on this issue.

When analysing an elastic crack tip stress–strain

* Corresponding author. Tel.: +91-22-550-5050 ext. 2586; fax: +91-22-550-5151.

E-mail addresses: nirmalk@apsara.barc.ernet.in (N.K. Mukhopadhyay), skmaiti@me.iitb.ernet.in (S.K. Maiti).

0045-7949/00/$ - see front matter
PII: S0045-7949(99)00209-6

Nomenclature

a	crack length
a_n	coefficients of traction
$B(m,n)$	Beta function
b_n	coefficients of displacement
c	singularity parameter
c_n	coefficients used in MCCI formulation
E	elastic modulus
G_{I}, G_{II}	strain energy release rates in modes I and II
h	length
K_{I}, K_{II}	stress intensity factors
l	crack tip element size
N_i, M_i	shape functions
p, q	components of crack edge loading normal and parallel to crack
r	distance from crack tip
s_j, t_j	components of traction parallel and normal to crack
u, v	components of displacement parallel and normal to crack
W	geometric dimensions of domain
W_{I}, W_{II}	crack closure work
x, y	Cartesian co-ordinates
Y	SIF correction factor
Δa	kink length
δ	distance from tip of kink to tip of short crack
θ	crack orientation with x-axis
ν	Poisson's ratio
ξ	natural co-ordinate
$\Gamma(m)$	Gamma function

field using the finite element method (FEM) based on the displacement formulation, the assumed displacement field is required to ensure only the strain singularity. The stress singularity is automatically guaranteed as stresses are calculated directly from the strains. Thus, there is no need for any special effort to ensure singularity in the stress. In contrast, in the BEM, the displacement and traction are treated as independent entities. The incorporation of singularity in, for example, the strain does not automatically guarantee the required singularity in traction.

The most common type of singularity encountered in stress analysis is the square root singularity. In 1976, Barsoum [9] introduced a special crack tip element, also known as "quarter point element", in the FEM, to model such a singularity. When the same element is employed in the BEM, it is able to partially model the singularity; the square root strain singularity is only ensured but not the square root traction singularity. The appropriate modelling of the singularities has received a considerable attention in the BEM [7,10–24]. In 1981, Blandford et al. [12], introduced a special element for modelling of both the singularities. This element is known as the 'traction singularity element'.

Though the SIFs can be evaluated through the most common displacement method, the modified crack closure integral (MCCI) technique offers better accuracy [25–28]. A procedure to calculate the SIFs based on the MCCI technique is given in detail for remote loading in [25,26], crack edge loading (e.g. fluid pressure) in [27] and thermal loading in [28]. It is relevant to note here that the conventional linear, quadratic and quarter point elements are used in the Ref. [26–28]. The effects of partial and total modelling of singularities while using the quarter point and traction singularity elements on the MCCI based computation of SIFs are discussed in [24]. Though the traction singularity element permits a total modelling of the singularities, this is helpful only for the case of square root singularity. At present there is no boundary element (BE) which can simulate variable order singularities partially or totally. The present paper has derived some motivation from this issue.

While the prime concern here has been the modelling of both the strain and traction singularities of variable order simultaneously, the effect of partial modelling of the strain singularity is also examined. Two variable singularity BEs are proposed. The element, which models only the variable strain singularity is termed here as Variable Strain Singularity (VSS) element. Similarly, the element which incorporates both the strain and traction singularities is termed as Variable Strain and Traction Singularity (VSTS) element. The use of MCCI in conjunction with the VSS and VSTS elements are also demonstrated.

When these special crack tip elements are employed, the evaluation of boundary integrals involves handling of product of two singularity terms. In such situations the integration can be as usual performed using the Gauss quadrature [6,8,29]. The order of Gauss quadrature has an influence on the

accuracy of the results. The degree of this influence is also elaborated.

2. Element formulation

2.1. Variable strain singularity (VSS) element

The usual shape functions for a 2D quadratic element are given by

$$N_1 = \xi(\xi-1)/2, \quad N_2 = \left(1-\xi^2\right) \quad \text{and} \quad N_3 = \xi(\xi+1)/2 \tag{1}$$

where ξ is the natural coordinate. The displacement and traction can be represented by the shape functions.

$$u = N_1u_1 + N_2u_2 + N_3u_3 \tag{2}$$

$$t = N_1t_1 + N_2t_2 + N_3t_3 \tag{3}$$

When the field variable (say, displacement) varies as $r^c\,(0<c<1)$, and the derivative of field variable (strain) as r^{c-1}, the order of singularity is $1-c$. The value $c = 0.5$ gives the common square root strain singularity. To develop an element with singularity at the crack tip, the element displacement shape functions can be manipulated. The slope of all the shape functions should be adjusted to give a value of infinity at the crack tip. At the same time the shape functions should also fulfil the rigid body and constant strain criteria. A set of such shape functions are given below.

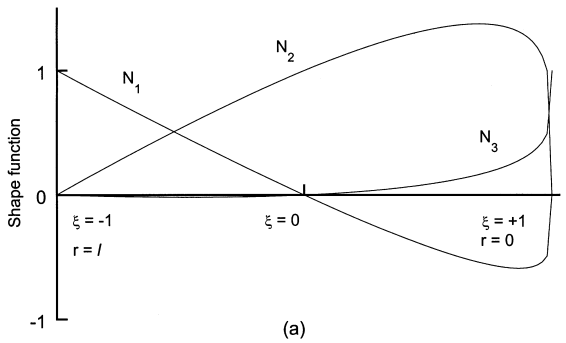

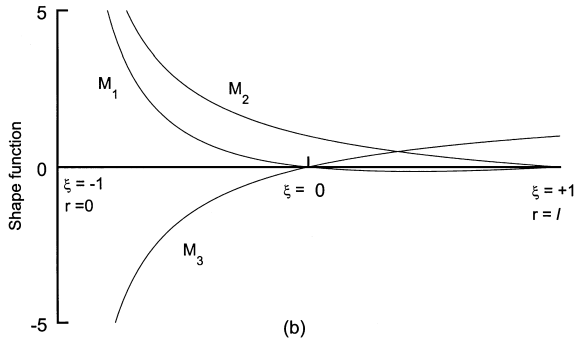

Fig. 1. (a) Displacement and traction shape functions for VSS element; displacement shape function for VSTS element. (b) Traction shape functions for VSTS element.

$$N_1 = 2^c\left[-(r/l)^c+(r/l)^{c+1}\right]+(r/l)$$

$$N_2 = 2^{c+1}\left[(r/l)^c-(r/l)^{c+1}\right]$$

$$N_3 = 2^c\left[-(r/l)^c+(r/l)^{c+1}\right]-(r/l)+1 \tag{4}$$

Here $r = l-x$ (Fig. 1a) and $r/l = (1-\xi)/2$. The modified shape functions have the following nodal values.

$$r/l = 0: \quad N_1 = 0, N_2 = 0, N_3 = 1$$

$$r/l = 1/2: \quad N_1 = 0, N_2 = 1, N_3 = 0$$

$$r/l = 1: \quad N_1 = 1, N_2 = 0, N_3 = 0 \tag{5}$$

The derivatives of the shape functions are

$$\frac{\partial N_1}{\partial x} = -\left(\frac{1}{l}\right)+2^c c\left(\frac{1}{l}\right)\left(\frac{l-x}{l}\right)^{c-1}-2^c(c+1)\left(\frac{1}{l}\right)\times\left(\frac{l-x}{l}\right)^c$$

$$\frac{\partial N_2}{\partial x} = -2^{c+1}c\left(\frac{1}{l}\right)\left(\frac{l-x}{l}\right)^{c-1}+2^{c+1}(c+1)\left(\frac{1}{l}\right)\times\left(\frac{l-x}{l}\right)^c$$

$$\frac{\partial N_3}{\partial x} = \left(\frac{1}{l}\right)-2^c c\left(\frac{1}{l}\right)\left(\frac{l-x}{l}\right)^{c-1}+2^c(c+1)\left(\frac{1}{l}\right)\times\left(\frac{l-x}{l}\right)^c \tag{6}$$

It may be noted that all the derivatives display r^{c-1} singularity at $r = 0$. The displacement field can now be written by adapting these shape functions. If the traction is expressed through the same shape functions, it does not display any singularity. Such an element is an example of the VSS element.

It can be easily verified that $\sum N_i = 1$. This satisfies the rigid body criteria. The proposed element fulfils the constant strain criteria. This is checked in the follow-

ing. Consider a situation that the temperature of the element is uniformly raised by T keeping the node 3 fully restrained. This gives rise to displacements $u_1 = l\alpha T$ and $u_2 = l\alpha T/2$, where α is the coefficient of thermal expansion. The element strain, on substitution,

$$\frac{\partial u}{\partial x} = u_1 \frac{\partial N_1}{\partial x} + u_2 \frac{\partial N_2}{\partial x} = \alpha T \tag{7}$$

The element therefore passes the constant strain requirement.

2.2. Variable strain and traction singularity (VSTS) element

To model the singularity behaviour fully, separate shape functions are needed to incorporate the variable traction singularity. The new shape functions can be formed with the help of the derivatives of the shape functions associated with the VSS element. A set of such shape functions are given below.

$$M_1 = 2^c\left[(l/r)^{1-c} - (r/l)^c\right] + 2(r/l) - 2$$

$$M_2 = 2^c\left[(l/r)^{1-c} - (r/l)^c\right]$$

$$M_3 = 2^c\left[-(l/r)^{1-c} + (r/l)^c\right] + 1 \tag{8}$$

where $r = x$ (Fig. 1b) and $r/l = (1+\xi)/2$.

The modified shape functions have the following nodal values.

$$r/l = 0: \quad M_1 = \lim_{r\to 0}(l/r)^{1-c}, \quad M_2 = \lim_{r\to 0}(l/r)^{1-c},$$

$$M_3 = \lim_{r\to 0}(l/r)^{1-c}$$

$$r/l = 1/2: \quad M_1 = 0, \quad M_2 = 1, \quad M_3 = 0$$

$$r/l = 1: \quad M_1 = 0, \quad M_2 = 0, \quad M_3 = 1 \tag{9}$$

All the shape functions ensure an $(1-c)$ singularity at the crack tip ($r\to 0$). The required variation of traction over the element can therefore be presented by

$$t = t_1 M_1 + t_2 M_2 + t_3 M_3 \tag{10}$$

A simultaneous representation of displacement and traction fields by Eqs. (4) and (10) respectively gives a VSTS element.

Adoption of the two new elements in an existing standard boundary element programme is a straightforward matter. However, a proper care must be taken in evaluating the terms of $[H]$ and $[G]$ matrices, where $[H]\{u\} = [G]\{t\}$. Particularly, when both the load and field points are in the special singularity element, the origins ($r = 0$) are different for the displacement and traction fields.

3. MCCI based computation of stress intensity factors

The SIFs at the tip of an elastic crack can be determined through a direct comparison of displacements of the node closest to the crack tip. The accuracy of the SIFs can be improved if the calculations are done through the energy release rates. One of the important methods to evaluate the strain energy release rate is Irwin's crack closure integral (CCI). It is first adapted by Rybicki and Kanninen [30]. They described the method considering a linear variation of the displacement field around the crack tip. Consequently the element ensures a constant strain field. They termed the method as modified crack closure integral (MCCI) technique. Later it has been shown by many investigators (e.g. Maiti [31]) that crack line displacement and stresses can be locally smoothed using the computed nodal data. These smoothed field can then be employed to compute the crack closure work. Recently the effectiveness of this method is also demonstrated in BEM [25–28] only in relation to linear, quadratic and quarter point elements around the crack tip.

The energy release rate associated with a crack extension in a given mode is equal to the work done in closing an infinitesimal extended crack back to its original length. For a crack subjected to remote mechanical loading the crack closure work done can be calculated.

$$W_{\mathrm{I}} = \frac{1}{2}\int_0^l v\, t\, \mathrm{d}x \tag{11}$$

where, G_{I} is the crack closure work in mode I, v is the crack opening displacement, t is the traction and l is the infinitesimal virtual crack extension. The origin is located at the crack tip and the axis x is oriented in the direction of the crack extension. In the BEM, it has been shown that an assumption of the crack opening behind, and traction ahead of, the crack tip as per initially assumed variations (e.g. quadratic for quadratic element) helps in improving the accuracy [26]. l is generally taken equal to the crack tip element size. The mode I strain energy release rate (SERR) G_{I} can be obtained from the crack closure work ($G_{\mathrm{I}} = W_{\mathrm{I}}/l$). In this method the component modes (G_{I} and G_{II}) can be separated. The SIFs can be derived from the SERRs. Close form relations to evaluate SIFs from the computed displacements and tractions for linear, quadratic and quarter point elements for remote mechanical loading is available in [26].

Loading on the crack edges come up due to explicit mechanical loading, e.g., crack subjected to fluid press-

ure, etc. In such a case, when a crack extends or an extended crack is closed, it must be noted that there is an extra loading on the newly formed crack edges on top of the usual crack closure forces. This loading contributes to an additional amount of work. A crack closure integral calculation must therefore cognise this fact. In such situations the crack closure work have two parts. One part is due to the usual tractions and the other is due to the fluid pressure p. For a mode I problem the crack closure work is given by

$$W_{\mathrm{I}} = \frac{1}{2}\int_0^l v\, t\, \mathrm{d}x + \frac{1}{2}\int_0^l v\, p\, \mathrm{d}x \tag{12}$$

The mode II crack closure work W_{II} can be evaluated in a similar way. Relations for the SIFs for linear, quadratic and quarter point elements around the crack tip are available in [27].

3.1. VSS element

In this element the opening displacement and traction variations are given by

$$v = b_1(1-x/l)^c + b_2(1-x/l)^{c+1} + b_3(1-x/l) + b_4 \tag{13}$$

$$t = a_1(x/l)^c + a_2(x/l)^{c+1} + a_3(x/l) + a_4 \tag{14}$$

where $b_1 = (-2^c v_{j-2} + 2^{c+1} v_{j-1} - 2^c v_j)$, $b_2 = (2^c v_{j-2} - 2^{c+1} v_{j-1} + 2^c v_j)$, $b_3 = (v_{j-2} - v_j)$, $b_4 = v_j$ and $a_1 = (-2^c t_{j+2} + 2^{c+1} t_{j+1} - 2^c t_j)$, $a_2 = (2^c t_{j+2} - 2^{c+1} t_{j+1} + 2^c t_j)$, $a_3 = (t_{j+2} - t_j)$ and $a_4 = t_j$. The terms v_j and t_j are the displacement and traction in the direction normal to the crack.

3.1.1. Remote mechanical loading

For this type of loading the mode I crack closure work is obtained from Eq. (11). The displacement and traction are as per Eqs. (13) and (14). For a symmetric crack configuration, $v_j = 0$. For other cases, displacements relative to the crack tip is to be considered. Combining Eqs. (11), (13) and (14)

$$\begin{aligned} W_{\mathrm{I}} = \frac{l}{2}\int_0^1 \big\{ & (1-z)^c z^c a_1 b_1 + (1-z)^{c+1} z^c a_1 b_2 \\ & + (1-z) z^c a_1 b_3 + (1-z)^c z^{c+1} a_2 b_1 \\ & + (1-z)^{c+1} z^{c+1} a_2 b_2 + (1-z) z^{c+1} a_2 b_3 \\ & + (1-z)^c z a_3 b_1 + (1-z)^{c+1} z a_3 b_2 \\ & + (1-z) z a_3 b_3 + (1-z)^c a_4 b_1 \\ & + (1-z)^{c+1} a_4 b_2 + (1-z) a_4 b_3 \big\}\, \mathrm{d}z \end{aligned} \tag{15}$$

where $z = x/l$. Finally, the mode I strain energy release rate $G_{\mathrm{I}} = W_{\mathrm{I}}/l$ is obtained.

$$\begin{aligned} G_{\mathrm{I}} = \big[& v_{j-2}(c_1 a_1 + c_2 a_2 + c_3 a_3 + c_4 a_4) + v_{j-1}(c_5 a_1 \\ & + c_6 a_2 + c_7 a_3 + c_8 a_4) \big]/2 \end{aligned} \tag{16}$$

where

$$\begin{aligned} c_1 &= \big[-2^c B(1+c, 1+c) + 2^c B(2+c, 1+c) \\ &\quad + B(2, 1+c) \big], \\ c_2 &= \big[-2^c B(1+c, 2+c) + 2^c B(2+c, 2+c) \\ &\quad + B(2, 2+c) \big], \\ c_3 &= \big[-2^c B(1+c, 2) + 2^c B(2+c, 2) + B(2, 2) \big], \\ c_4 &= \big[-2^c/(1+c) + 2^c/(2+c) + 0.5 \big], \\ c_5 &= \big[2^{c+1} B(1+c, 1+c) - 2^{c+1} B(2+c, 1+c) \big], \\ c_6 &= \big[2^{c+1} B(1+c, 2+c) - 2^{c+1} B(2+c, 2+c) \big], \\ c_7 &= \big[2^{c+1} B(1+c, 2) - 2^{c+1} B(2+c, 2) \big], \\ c_8 &= \big[2^{c+1}/(1+c) - 2^{c+1}/(2+c) \big], \end{aligned} \tag{17}$$

and

$$B(m, n) = \int_0^1 (1-z)^{m-1} z^{n-1}\, \mathrm{d}z \tag{18}$$

A similar expression can also be derived for a mode II crack. That is,

$$\begin{aligned} G_{\mathrm{II}} = \big[& u_{j-2}(c_1 a_1 + c_2 a_2 + c_3 a_3 + c_4 a_4) + u_{j-1}(c_5 a_1 \\ & + c_6 a_2 + c_7 a_3 + c_8 a_4) \big]/2 \end{aligned} \tag{19}$$

where u is the crack sliding displacement. In defining a_i's tractions s_j, s_{j+1} and s_{j+2} must be used in place of t_j, t_{j+1} and t_{j+2}, respectively.

3.1.2. Crack edge pressure loading

For fluid pressure acting on the crack edges, the crack closure work is as per Eq. (12). Following the procedure as given in [27], final expression for the mode I and mode II energy release rates are obtained in the form

$$G_{\mathrm{I}} = \big[v_{j-2}(c_1a_1 + c_2a_2 + c_3a_3 + c_4a_4 + c_4p) + v_{j-1}(c_5a_1 + c_6a_2 + c_7a_3 + c_8a_4 + c_8p)\big]/2 \quad (20)$$

$$G_{\mathrm{II}} = \big[u_{j-2}(c_1a_1 + c_2a_2 + c_3a_3 + c_4a_4 + c_4q) + u_{j-1}(c_5a_1 + c_6a_2 + c_7a_3 + c_8a_4 + c_8q)\big]/2 \quad (21)$$

The constants a_i's and c_i's are already defined.

3.2. VSTS element

In this element the traction is given by

$$t = a_1(l/x)^{1-c} + a_2(x/l)^c + a_3(x/l) + a_4 \quad (22)$$

where $a_1 = (-2^c t_{j+2} + 2^c t_{j+1} + 2^c t_j)$; $a_2 = (2^c t_{j+2} - 2^c t_{j+1} - 2^c t_j)$; $a_3 = 2t_j$ and $a_4 = (t_{j+2} - 2t_j)$. The opening displacement field can be represented by Eq. (13).

Following the procedure given for the energy calculation for the VSS element, the mode I and mode II strain energy release rates for remote mechanical loading for this can be obtained. Explicitly

$$G_{\mathrm{I}} = \big[v_{j-2}(c_1a_1 + c_2a_2 + c_3a_3 + c_4a_4) + v_{j-1}(c_5a_1 + c_6a_2 + c_7a_3 + c_8a_4)\big]/2 \quad (23)$$

$$G_{\mathrm{II}} = \big[u_{j-2}(c_1a_1 + c_2a_2 + c_3a_3 + c_4a_4) + u_{j-1}(c_5a_1 + c_6a_2 + c_7a_3 + c_8a_4)\big]/2 \quad (24)$$

where

$$c_1 = \big[-2^c B(1+c, c) + 2^c B(2+c, c) + B(2, c)\big],$$

$$c_2 = \big[-2^c B(1+c, 1+c) + 2^c B(2+c, 1+c) + B(2, 1+c)\big],$$

$$c_3 = \big[-2^c B(1+c, 2) + 2^c B(2+c, 2) + B(2, 2)\big],$$

$$c_4 = \big[-2^c/(1+c) + 2^c/(2+c) + 0.5\big],$$

$$c_5 = \big[2^{c+1} B(1+c, c) - 2^{c+1} B(2+c, c)\big],$$

$$c_6 = \big[2^{c+1} B(1+c, 1+c) - 2^{c+1} B(2+c, 1+c)\big],$$

$$c_7 = \big[2^{c+1} B(1+c, 2) + 2^{c+1} B(2+c, 2)\big],$$

$$c_8 = \big[2^{c+1}/(1+c) - 2^{c+1}/(2+c)\big] \quad (25)$$

For a crack edge pressure loading and/or remote mechanical loading G_{I} and G_{II} are as follows.

$$G_{\mathrm{I}} = \big[v_{j-2}(c_1a_1 + c_2a_2 + c_3a_3 + c_4a_4 + c_4p) + v_{j-1}(c_5a_1 + c_6a_2 + c_7a_3 + c_8a_4 + c_8p)\big]/2 \quad (26)$$

$$G_{\mathrm{II}} = \big[u_{j-2}(c_1a_1 + c_2a_2 + c_3a_3 + c_4a_4 + c_4q) + u_{j-1}(c_5a_1 + c_6a_2 + c_7a_3 + c_8a_4 + c_8q)\big]/2 \quad (27)$$

where the coefficients a_i and c_i are given by Eqs. (22) and (25), respectively.

3.3. Evaluation of SIFs

The coefficients c_n are evaluated using

$$B(m, n) = \Gamma(m)\Gamma(n)/\Gamma(m+n) \quad (28)$$

$$\Gamma(n) = \lim_{j\to\infty} \frac{j!j^n}{n(n+1)(n+2)\dots(n+j)}, \quad n \neq 0, -1, -2, \dots \quad (29)$$

For a particular c, the gamma function is calculated using double precision arithmetic and $j = 50{,}000$. It must be emphasised that the SIFs can be evaluated from G_{I} and G_{II} as their correlations are known only for $c = 0.5$. In other cases the MCCI based relations can be employed just to calculate the strain energy release rates.

4. Case studies

Three case studies, involving mode I or mixed mode crack subjected to mechanical loading, are presented. The computation is performed on a PC486 using single precision arithmetic.

4.1. Pressurised crack normal to bimaterial interface

This example deals with a crack normal to, and terminating at, a bimaterial interface (Fig. 2a). The singularity at the embedded crack tip C is square root singularity ($c = 0.5$). The order of singularity of crack tip which lies at the bimaterial interface D is dependent on the material combination and the state of stress [2]. Here the material combination, aluminium and epoxy, is studied under a state of plane strain. The selected material properties for aluminium are: elastic modulus $E = 68.95$ GPa (10^7 psi) and Poisson's ratio $\nu = 0.3$. For epoxy the same properties are: $E = 3.102$ GPa

(0.45×10^6 psi) and $\nu = 0.35$. When the crack is located in aluminium, the ratio of shear modulus $m = 0.043$ and $c = 0.1752$. In the reverse case $m = 23.08$ and $c = 0.6619$. The major domain dimensions are $a/W = L/W = 1/9$ and $W = 228.6$ mm (9 in.). The crack is subjected to a fluid pressure of $p = 6.895$ kPa (1 psi).

Half of the plate is discretised because of the symmetry (Fig. 2b). The boundary integral equations are considered separately for each material and they are matched at the interface. Total 59 elements are employed. The element size at C is $2\%a$. The subsequent element sizes are $0.08a$, $0.2a$, etc. The mesh near D is kept relatively finer. The crack tip element size is $0.01a$, the subsequent element sizes are $0.02a$, $0.04a$, $0.08a$, etc. The problem is studied by employing both the VSS and the VSTS elements. The variable singularity elements are considered at both the crack tips. However, for the crack tip C, c is 0.5 and for D an appropriate value of c is specified. This case has earlier been studied by Cook and Erdogan [2] using singularity integral equation. Tracey and Cook [3] and Maiti [5] have reported results based on the special variable order singularity finite elements.

The normalised crack opening displacement (COD) v/a plotted as a function of distance from D is com-

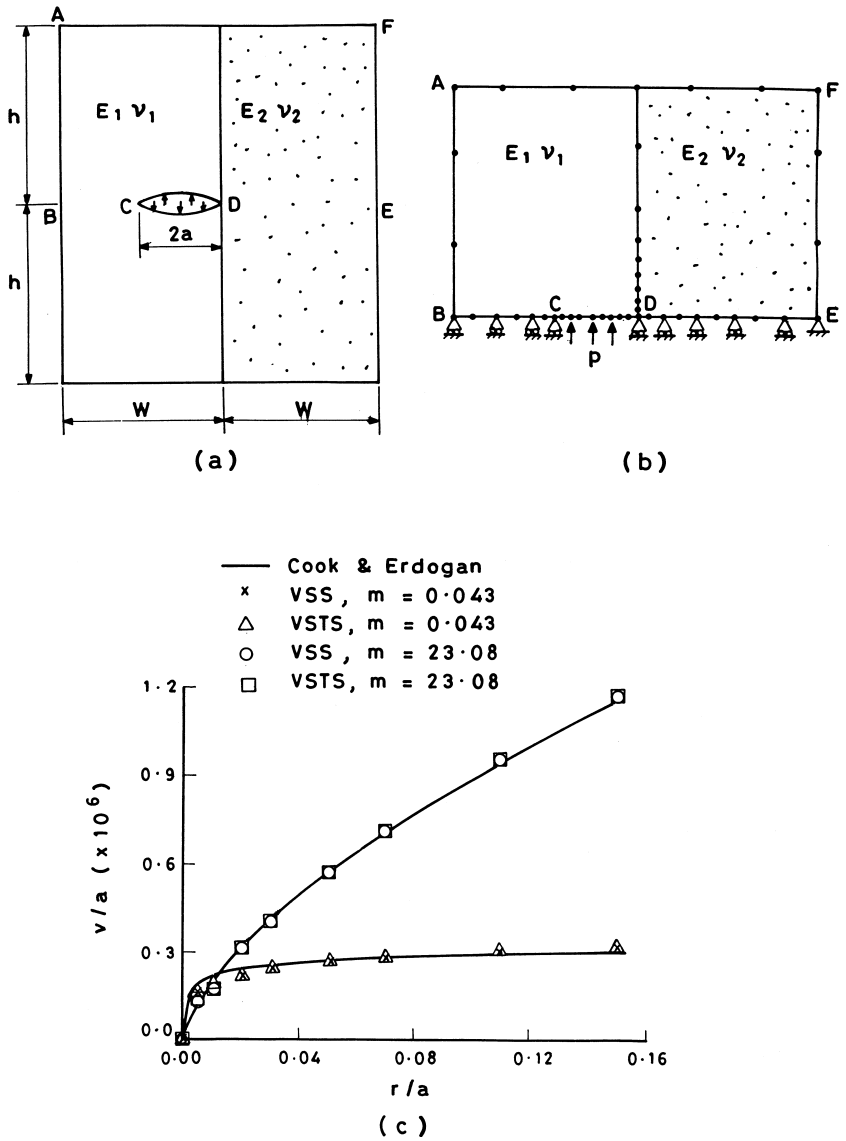

Fig. 2. (a) Pressurised crack at bimaterial interface. (b) Boundary element mesh. (c) Comparison of crack opening displacements.

Table 1
Comparison of SIF correction factor Y at interface crack tip for crack under fluid pressure by displacement method

m	Cook and Erdogan [2]	Tracey and Cook [3]	Maiti [5]	Present calculation		
				Quadratic	VSS	VSTS
0.043	0.048	0.0528 (9.97)[a]	0.049 (2.08)	0.0418 (−12.92)	0.0438 (−8.75)	0.0471 (−1.875)
23.07		4.123	4.047	4.078	4.073	4.096

[a] % difference with Cook and Erdogan's results.

pared with that of Cook and Erdogan [2] (Fig. 2c). For $m = 23.08$, the CODs agree closely. In this case the results by the VSS and VSTS are nearly the same. For $m = 0.043$, the computed displacement near the bimaterial interface is less than that of Cook and Erdogan [2] solution for $r/a < 0.01$. However, for $r/a > 0.01$, the agreement is again good. The difference in the crack opening displacement (COD) for $r/a < 0.01$ is more in the case of VSS element than in the case of VSTS element.

The SIFs at C have been evaluated using both the displacement [3] and the MCCI based method. The displacement of the second corner node instead of the first corner node, if considered for the displacement based calculations of the SIFs, gives as usual [26,27] more accurate results. The MCCI based results are obtained by Eq. (20). For D the SIF is calculated based only on the displacement method. In case of $m = 0.043$, the SIF correction factor $Y (Y = K_I/p(\pi a)^{1-c})$ at D differ from the Cook and Erdogan's [2] solution by 8.75% (Table 1) when the VSS element is employed. However, the difference reduces to 1.875% in the case of VSTS element. The difference obtained by Tracey and Cook [3] and Maiti [5] are 9.97% and 2.08%, respectively. For $m = 23.08$, the computed Y for both the elements match closely with the results of Tracey and Cook [3]. For C, the calculated Y's ($Y's = K_I/p\sqrt{(\pi a)}$) using displacement and MCCI technique are shown in Table 2. In general, for $m = 0.043$, the present results differ with Cook and Erdogan's [2] analytical solutions but are very close to that of Tracey and Cook's [3] finite element solutions. It is relevant to note that Tracey and Cook have reported a difference of 12.17% with Cook and Erdogan's solutions. For $m = 23.08$, the results are close to the solutions of both Cook and Erdogan [2] and Tracey and Cook [3]. The Y's are also evaluated at the interface using ordinary quadratic elements (Table 1). The computed Y for $m = 0043$ differ from the reference solution by 12.92%. Therefore, it is clear that modelling of the singularity improves the accuracy of the results.

The influence of order of Gauss quadrature [29] on accuracy of Y, for $m = 23.08$ has been examined (Table 3). Irrespective of the element the accuracy of the SIF is not that significantly affected by the order of integration if the computation is based on the displacement method. The accuracy is significantly affected by the order of integration in the case of VSTS element when the computation is based on the MCCI method; an order higher than 10 is generally permissible. The MCCI method in conjunction with the VSS element gives a very good accuracy with order of integration even less than 10.

4.2. Kinked crack–short crack interaction under mode I loading

A kinked crack in a flat plate under uniformly distributed load is studied (Fig. 3a). The plate dimensions are $a/W = 0.25\sqrt{2}$, $h/W = 1.5$ and $W = 10$ mm. Two different kink (AB) sizes of $\Delta a/W = 0.0125$ and 0.025

Table 2
Comparison of SIF correction factor Y at embedded crack tip for crack under fluid pressure by displacement method and MCCI

m	Cook and Erdogan [2]	Tracey and Cook [3]	Maiti [5]	VSS		VSTS	
				Displacement	MCCI	Displacement	MCCI
0.043	1.355	1.520 (12.17)[a]	1.490 (9.96)	1.461 (7.82)	1.497 (10.48)	1.479 (9.15)	1.527 (12.69)
23.07	0.882	0.890 (0.91)	0.876 (−0.68)	0.854 (−3.17)	0.892 (1.13)	0.859 (−2.61)	0.904 (2.49)

[a] % difference with Cook and Erdogan's results.

Table 3
Effect of order of Gauss quadrature on SIF correction factor Y for epoxy aluminium bimaterial strip (crack in epoxy)

Order of quadrature	$Y = K_I/p\sqrt{(\pi a)}$ at embedded crack tip by				$Y = K_I/p(\pi a)^{1-c}$ at interface crack tip by	
	VSS		VSTS		VSS	VSTS
	Displacement	MCCI	Displacement	MCCI	Displacement	Displacement
4	0.8535 (−3.233)[a]	0.8957 (1.549)	0.8579 (−2.732)	0.9790 (10.995)	4.073	4.092
8	0.8535 (−3.233)	0.8922 (1.162)	0.8581 (−2.706)	0.9258 (4.969)	4.073	4.093
10	0.8536 (−3.220)	0.8920 (1.131)	0.8583 (−2.686)	0.9166 (3.924)	4.073	4.094
12	0.8536 (−3.220)	0.8918 (1.115)	0.8585 (−2.667)	0.9107 (3.254)	4.073	4.094
16	0.8536 (−3.220)	0.8918 (1.106)	0.8587 (−2.641)	0.9036 (2.448)	4.073	4.096

[a] % difference with Cook and Erdogan's results.

have been considered. The crack angle θ is 45°. The material properties are: $E = 210$ GPa and $\nu = 0.3$. The singularity parameter c is 0.674 at A and 0.5 at B. There is no singularity at the re-entrant corner. The plate is subjected to a uniform tension $\sigma = 10$ MPa. Subregion technique is adapted for the analysis. Each region is modelled using 23 quadratic elements (Fig. 3b). The elements surrounding A and B are the variable order singularity elements of size $\Delta a/2$. A state of plane stress is assumed.

This problem is again studied using both the VSS and the VSTS elements. The SIF correction factors Y, $Y = K_I/\sigma\sqrt{\pi(a + \Delta a)}$, at B are computed through the MCCI method (Table 4). This problem has earlier been studied by Tracey and Cook [3] and Maiti [5]. The maximum difference from the reference solution [3] is 0.402% for the VSS element and 0.968% for the VSTS element. The finite element solutions of Tracey and Cook [3] differ by around 4%. The solutions presented by Maiti [5] employing variable order singularity finite element differ by 0.9%. The crack tip element size used by Maiti [5] is $\Delta a/2$. In this case also, the VSS and the VSTS elements perform better than ordinary quadratic elements (Table 4). The maximum difference from reference solution is 2% when quadratic elements are employed. The mode II SIF is, as expected, negligible.

The effect of variation of order of integration on the accuracy of SIFs for the kinked crack problem is shown in Table 5. The order is varied from 4 to 16. For the VSS element, the accuracy almost stabilises to around 10. For the VSTS element the accuracy increases as the order of integration increases. For this case, a higher order integration is preferable.

The effect of interaction between a short crack and a kinked crack ($\Delta a/W = 0.0125$) has been studied (Fig. 3c). A parametric study has been done by varying short crack length $2l$ and keeping Δa and inter-crack distance δ constant. $\Delta a/2l$ is varied from 0.125 to 1. The mesh employed is similar to the previous (Fig. 3b) one; each region is modelled by 27 elements. The crack tip element sizes surrounding A and B are $\Delta a/2$. The distance δ is modelled with two elements. Four elements of uniform size are employed to model the short crack in each case. The SIF correction factor Y at B is computed by both the VSS and the VSTS elements through the MCCI technique (Table 6). For a value of $2l/\Delta a = 8$, Y is nearly 47% more than the corresponding value in the absence of crack $2l$. As this crack length ($2l$) reduces, Y

Table 4
Comparison of SIFs for kinked crack (Fig. 3a)

$\Delta a/W$	Mode	Reference solution [3]	Tracey and Cook [3]	SIF correction factor Y by		
				Ordinary	VSS	VSTS
0.0125	I	1.542	1.480 (−4.0)[a]	1.5736 (2.05)	1.5447 (0.174)	1.5555 (0.874)
0.0125	II	0.0	0.0015	0.0027	0.0024	0.0022
0.025	I	1.581	1.518 (−4.0)	1.6123 (1.98)	1.5873 (0.402)	1.5963 (0.968)
0.025	II	0.0	0.0015	0.0077	0.0043	0.0016

[a] Difference with reference solution.

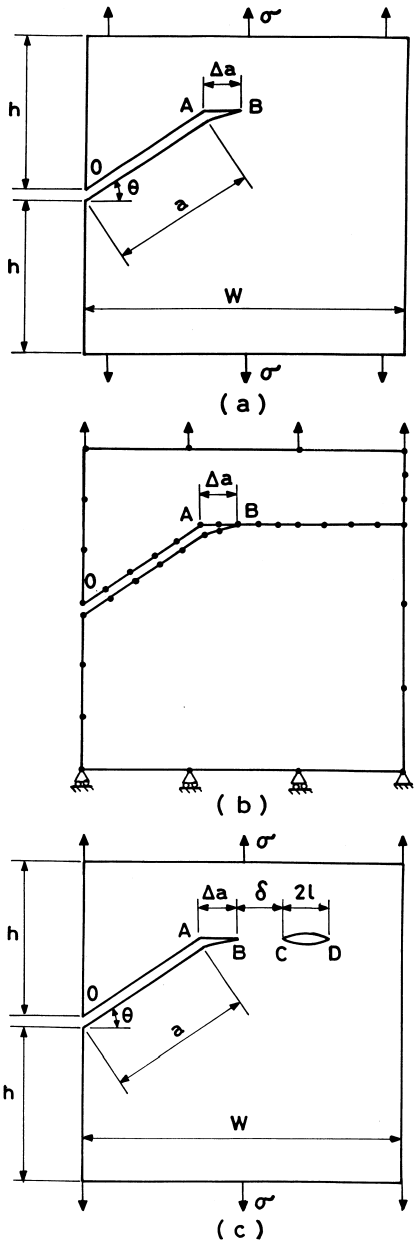

Fig. 3. (a) Kinked crack under mode I loading. (b) Boundary element mesh. (c) Kinked crack-short crack interaction.

decreases. When $2l = \Delta a$, Y reduces to the Y of the kinked crack (Y_{kink}).

The effect of δ (Fig. 4) on Y has been examined. As the inter-crack distance is reduced, the increase in Y is more pronounced. As an example, for $\Delta a/2l = 0.125$, when δ is reduced to $\Delta a/4$, the increase in Y is around 120% of the Y_{kink}. Even for $\Delta a/2l = 1$, Y is more than Y_{kink} by about 18%.

4.3. Kinked crack–short crack interaction under mixed mode loading

The problem is shown in Fig. 5a. The dimensions are: $a = 0.5h$, $h/W = 1.5$, $W = 20$ mm and $\theta = 30^\circ$. Other data are: $E = 210$ GPa, $\nu = 0.3$ and $\sigma = 10$ MPa. The order of singularity at the crack tip B is the usual square root singularity. The order of singularity at the knee A changes with the knee angle θ [1]. For $\theta = 30^\circ$; $c = 0.751975$. Initially a kink length of $\Delta a = 1\% a$ is considered and $\delta = \Delta a$. A short crack of length $2l$ (CD) is considered at a distance δ ahead of B in same alignment (Fig. 5a). The short crack length $2l$ is varied from $\Delta a/2l = 0.125$ to 1 keeping δ and $2l$ constant. The subregion technique is employed and each region is modelled by 27 elements. The crack tips A, B, C and D are surrounded by the variable order singularity elements. The size of crack tip elements at A and B is $\Delta a/2$. The inter-crack distance δ is modelled with two elements. Four elements of uniform size are employed to model CD. The SIF correction factor Y, $Y = K_{\text{I}}/\sigma\sqrt{(\pi a)}$, is computed at B by the VSS and VSTS elements through the MCCI technique (Table 7). No data is available in literature for a comparison in this case. For $2l = 8\Delta a$, the mode I and mode II SIF correction factors at B are 39% and 44% more than the corresponding Y_{kink} of Cotterell and Rice [32]. As

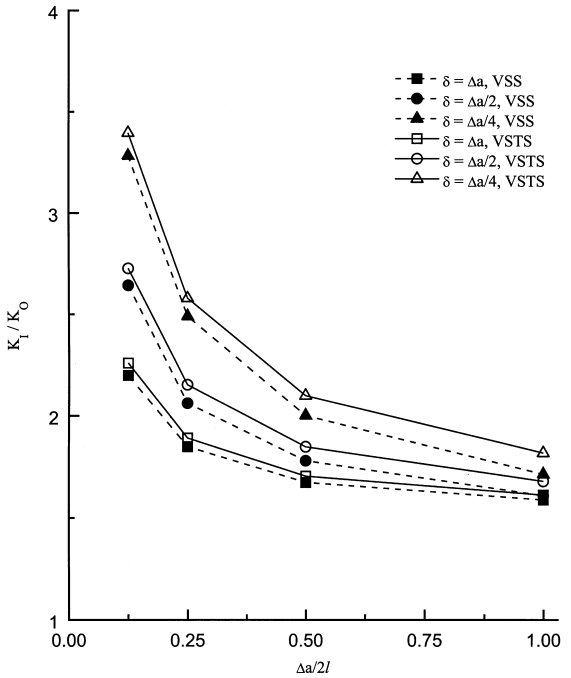

Fig. 4. Effect of short crack on kinked crack under mode I loading.

Table 5
Effect of variation of Gauss quadrature on accuracy of SIFs for kinked crack (Fig. 3a)

Reference solution [3]	Order of quadrature	Element			
		VSS		VSTS	
		Y	% difference	Y	% difference
		$\Delta a/W = 0.0125$			
	4	1.552	0.644	1.697	10.053
	8	1.546	0.229	1.601	3.848
1.542	10	1.545	0.199	1.585	2.788
	12	1.545	0.186	1.570	1.845
	16	1.545	0.174	1.556	0.874
		$\Delta a/W = 0.025$			
	4	1.595	0.870	1.745	10.402
	8	1.588	0.453	1.647	4.185
1.581	10	1.588	0.427	1.631	3.128
	12	1.588	0.413	1.616	2.218
	16	1.587	0.402	1.596	0.968

Table 6
Effect of kinked crack–short crack interaction on SIF correction factor Y at kink tip (Fig. 3c)

$\Delta a/2l$	SIF Correction Factor Y for					
	VSS			VSTS		
	$\delta = \Delta a$	$\delta = \Delta a/2$	$\delta = \Delta a/4$	$\delta = \Delta a$	$\delta = \Delta a/2$	$\delta = \Delta a/4$
0.125	2.199	2.643	3.282	2.260	2.727	3.395
0.250	1.850	2.063	2.491	1.892	2.154	2.580
0.500	1.675	1.781	2.002	1.705	1.849	2.100
1.000	1.589	1.610	1.714	1.613	1.680	1.819

Table 7
Effect of short crack–kinked crack interaction on SIF correction factor Y at kinked crack tip for mixed mode loading (Fig. 5a)

$\Delta a/2l$	Mode	SIF correction factor Y for					
		VSS element			VSTS element		
		$\Delta a = 4\%a$	$\Delta a = 2\%a$	$\Delta a = 1\%a$	$\Delta a = 4\%a$	$\Delta a = 2\%a$	$\Delta a = 1\%a$
0.125	I	3.8017	3.6238	3.4653	3.9036	3.7197	3.5648
0.125	II	1.0846	1.0074	0.9554	1.1130	1.0365	0.9896
0.250	I	3.2579	3.1011	2.9982	3.3360	3.1774	3.0831
0.250	II	0.9103	0.8546	0.8198	0.9331	0.8797	0.8514
0.500	I	2.9463	2.8211	2.7413	3.0088	2.8847	2.8163
0.500	II	0.8168	0.7732	0.7456	0.8358	0.7951	0.7751
1.000	I	2.7978	2.6880	2.5795	2.8500	2.7424	2.6383
1.000	II	0.7732	0.7351	0.7015	0.7892	0.7542	0.7280

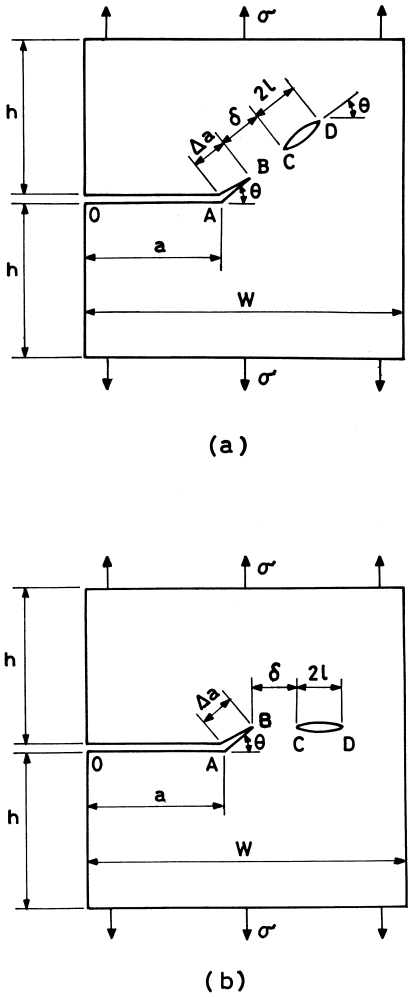

Fig. 5. Kinked crack-short crack interaction under mixed mode loading. (a) Short crack in alignment. (b) Short crack out of alignment.

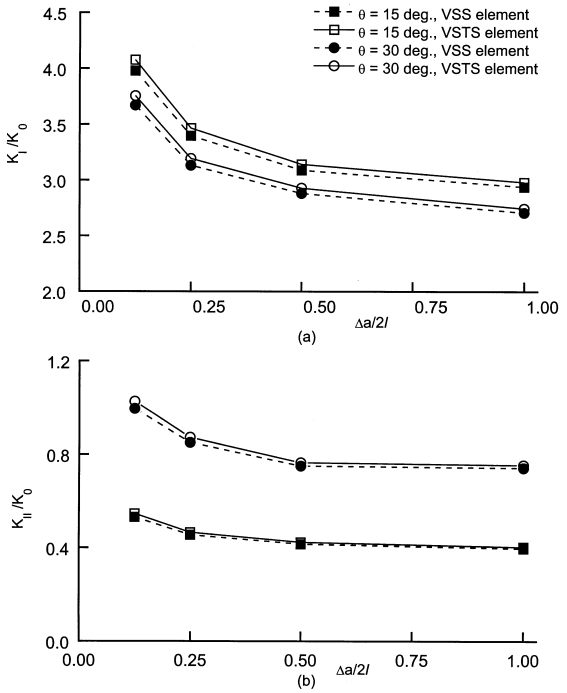

Fig. 6. Effect of short crack-kinked crack interaction on SIF correction factor at kinked crack tip for mixed mode loading (Fig. 5b). (a) Variation of mode I SIF. (b) Variation of mode II SIF.

the short crack length $2l$ reduces, Y decreases. For $2l = \Delta a$, Y at B approaches Y_{kink}. The kink length is varied to 2%a and 4%a and results are also presented in Table 7. In these cases also $\delta = \Delta a$ and $\Delta a/2l$ is varied from 0.125 to 1. The mode I and mode II Y's at B increase by 52% and 62% from Y_{kink} for $\Delta a = 4\%a$ and $\Delta a/2l = 0.125$. For $2l = \Delta a$, the Y's are more than Y_{kink} by 11% and 15%, respectively.

The effect of a out of alignment short crack located horizontally ahead of the kinked crack under mixed mode loading had also been studied (Fig. 5b). Two crack angles $\theta = 15^\circ$ ($c = 0.85733$) and 30° ($c = 0.751975$) are considered. Other data include $\Delta a = 2\%a$ and $\delta = \Delta a$. The short crack length $2l$ is varied from $\Delta a/2l = 0.125$ to 1. Similar nodal arrangements as in the earlier case but with slight readjustment of coordinates are employed. The variation of SIF correction factor Y at B is shown in Fig. 6. No data is available in this case for a comparison. The mode I SIF correction factor Y is less influenced by $\Delta a/2l$ than the mode II correction factor. With increase in ($\Delta a/2l$), Y reduces. A similar trend is observed for all θ. For a case, $\theta = 15^\circ$ and $2l = 8\Delta a$, the mode I and mode II correction factors are 35% and 48%, respectively more than the corresponding SIFs at the kink tip in the absence of the second crack.

5. Discussion

Two new variable order singularity boundary elements are introduced. The first element, the variable singularity (VSS) element, partially models the singularity behaviour. It models only the variable order strain singularity near a crack tip. The second element, the variable strain and traction singularity (VSTS) element, can simulate the singularity in both strain and traction. These elements are easy to implement and do not pose any problem in the system of equations or in solving them. Relations are given to compute the SIF

based on the modified crack closure integral (MCCI) technique for both these elements and these are useful for the case of square root singularity at the crack tip. In other cases they can be used to compute the strain energy release rates G_I and G_{II}. Mode I and mixed mode examples under remote mechanical loading and crack edge loading are presented to demonstrate the performance of the elements and the usefulness of the MCCI technique. In general, the accuracy of SIFs calculation by the proposed method is higher than the displacement method. These elements have definite edge over ordinary quadratic elements in modelling variable order singularity and computation of SIFs.

The accuracy of the computed SIFs is dependent on order of Gauss quadrature. For the case of VSS element the fundamental solution is multiplied by $(r/l)^c$. The order of singularity in the fundamental solution for displacement is dependent on $[\ln(1/r) \times (r)^c]$. However, in the case of fundamental solution for traction this is dependent on $[(1/r) \times (r)^c]$. In the case of VSTS element, the fundamental solution for traction is multiplied by $(r/l)^c$; thereby making the order of singularity to depend on $[(1/r) \times (r)^c]$. The fundamental solution of displacement is multiplied by $(l/r)^{1-c}$. The order of singularity here is guided by $[\ln(1/r) \times (1/r)^{1-c}]$. The order of singularity in the case of VSTS element is more powerful than the case of the VSS element. It is observed that the computed tractions near the crack tip vary with the order of integration, though the displacements do not change much for the VSTS element. Hence, the SIF when computed by displacement method stabilises for a moderate integration order. When calculations are performed through the MCCI technique, a higher order integration, 10 or more, is required in the case of VSTS element compared with VSS element for same degree of accuracy. In general, the VSTS element seems to have an edge over the VSS element notwithstanding the requirement of a higher integration order.

6. Conclusions

The following conclusions are drawn.

1. The variable order singularity can be modelled by a boundary element through a simple manipulation of its shape functions.
2. There is an improvement in accuracy of results, when the crack tip singularities are appropriately modelled.
3. The partial modelling though acceptable through an element like VSS, for a better accuracy of the SIFs the full simulation of both the strain and traction singularities through the VSTS element is desirable.
4. Though the displacement is a versatile method for the computation of the SIFs, a further enhancement in the accuracy of the SIFs is possible through the MCCI. The MCCI method can be utilised in all cases to compute G_I and G_{II}. It can be helpful for evaluation of the SIFs only in the case of square root singularity.
5. The presence of a crack ahead of a principal crack results in an substantial increase in the SIF depending on the inter-crack distance and its size.

References

[1] Williams ML. Stress singularities resulting from various boundary conditions in angular corners of plates in extension. J Appl Mech ASME 1952;19:526–8.

[2] Cook TS, Erdogan F. Stresses in bonded material with a crack perpendicular to the interface. Int J Eng Sci 1972;10:677–97.

[3] Tracey DM, Cook TS. Analysis of power type singularities using finite elements. Int J Numer Meth Engng 1977;11:1225–33.

[4] Stern M. Families of consistent conforming elements with singular fields. Int J Numer Meth Engng 1979;14:409–21.

[5] Maiti SK. A finite element for variable order singularities based on the displacement formulation. Int J Numer Meth Engng 1992;33:1955–74.

[6] Brebbia CA, Dominguez J. Boundary elements: An introductory course. London: McGraw Hill, 1982.

[7] Zang WL, Gudmundson P. Contact problems of kinked cracks modelled by a boundary integral method. Int J Numer Meth Engng 1990;29:847–60.

[8] Becker AA. The boundary element method in engineering: A complete course. London: McGraw Hill, 1992.

[9] Barsoum RS. On the use of isoparametric finite elements in linear fracture mechanics. Int J Numer Meth Engng 1976;10:25–37.

[10] Cruse TA, Wilson RB. Advanced applications of boundary-integral equation methods. Nucl Engng Des 1978;46:223–34.

[11] Tan CL, Fenner RT. Elastic fracture mechanics analysis by the boundary integral equation method. Proc Roy Soc Lond 1979;A.369:243–60.

[12] Blandford GE, Ingraffea AR, Ligget JA. Two dimensional stress intensity factor computations using the boundary element method. Int J Numer Meth Engng 1981;17:387–404.

[13] Xanthis LS, Bernal MJM, Atkinson C. The treatment of singularities in the calculation of stress intensity factors using the boundary integral equation method. Comput Methods Appl Mech Eng 1981;26:285–304.

[14] Nadiri F, Tan CL, Fenner RT. Three-dimensional analyses of surface cracks in pressurised thick walled cylinders. Int J Pres Vessels Piping 1982;10:159–67.

[15] Martinez J, Dominguez J. On the use of quarter-point boundary elements for stress intensity factor computations. Int J Numer Meth Engng 1984;20:1941–50.

[16] Aliabadi MH, Rooke DP, Cartwright DJ. An improved boundary element formulation for calculating stress intensity factors: application to aerospace structures. J Strain Anal 1987;22:203–7.
[17] Gangming L, Yongyuan Z. Improvement of stress singular element for crack problems in three dimensional boundary element method. Engng Fract Mech 1988;31:993–9.
[18] Aliabadi MH, Rooke DP, Cartwright DJ. Fracture-mechanics weight-functions by the removal of singular fields using boundary element analysis. Int J Fract 1989;40:271–84.
[19] Watson JO. Singular boundary elements for the analysis of cracks in plane strain. Int J Numer Meth Engng 1995;38:2389–411.
[20] Chandra A, Huang Y, Wei X, Hu KX. A hybrid micro-macro BEM formulation for micro-crack clusters in elastic components. Int J Numer Meth Engng 1995;38:1215–36.
[21] Saez A, Gallego R, Domingeuz J. Hypersingular quarter-point boundary elements for crack problems. Int J Numer Meth Engng 1995;38:1681–701.
[22] Chen WH, Chen TC. An efficient dual boundary element technique for a two-dimensional fracture problem with multiple cracks. Int J Numer Meth Engng 1995;38:1739–56.
[23] Prasad NNV, Aliabadi MH, Rooke DP. Effect of thermal singularities on stress intensity factors: edge crack in rectangular and circular plate. Theo Applied Fract Mech 1996;24:203–15.
[24] Mukhopadhyay NK, Maiti SK, Kakodkar A. Effect of modelling of traction and thermal singularities on accuracy of SIFs computation through modified crack closure integral in BEM. Engng Fract Mech 1999;64:141–59.
[25] Farris TN, Liu M. Boundary element crack closure calculation of three-dimensional stress intensity factors. Int J Fract 1993;60:33–47.
[26] Mukhopadhyay NK, Maiti SK, Kakodkar A. Further considerations in modified crack closure integral based computation of stress intensity factor in BEM. Engng Fract Mech 1998;59:269–79.
[27] Mukhopadhyay NK, Maiti SK, Kakodkar A. BEM based evaluation of SIFs using modified crack closure integral technique under remote and/or crack edge loading. Engng Fract Mech 1998;61:655–71.
[28] Mukhopadhyay NK, Maiti SK, Kakodkar A. Modified crack closure integral based computation of SIFs for 2-D thermoelastic problems through BEM. Nucl Engng Des 1999;187:277–90.
[29] Stroud AH, Secrest D. Gaussian quadrature formulas. New York: Prentice-Hall, 1966.
[30] Rybicki EF, Kanninen MF. A finite element calculation of stress intensity factors by a modified crack closure integral. Engng Fract Mech 1977;9:931–8.
[31] Maiti SK. Finite element computation of crack closure integrals and stress intensity factors. Engng Fract Mech 1992;41:339–48.
[32] Cotterell B, Rice JR. Slightly curved or kinked cracks. Int J Fract 1980;16:155–69.